Numerical simulation of laser ultrasound detection of small defect in metal plates

Jianfei Guan (关建飞)[1], Zhonghua Shen (沈中华)[1], Jian Lu (陆 建)[1], Xiaowu Ni (倪晓武)[1], Jijun Wang (王纪俊)[1,2], and Baiqiang Xu (许伯强)[2]

[1]*Department of Applied Physics, Nanjing University of Science and Technology, Nanjing 210094*
[2]*Faculty of Science, Jiangsu University, Zhenjiang 212013*

In order to further confirm the relations between the size of internal defect and the measured ultrasonic signals and understand the interaction mechanism between the ultrasonic wave and inside defect, this paper has constructed the two-dimensional (2D) plane strain finite element model of the Al plate with the inside defect to simulate the scattering process of the ultrasonic wave generated by the pulsed laser in the Al specimen. The dependence of the normalized amplitude of the defect signal on the defect diameter has been calculated in details, and the ultrasonic reflectance by the cylindrical shaped internal defect was evaluated in details using the numerical results. It is demonstrated that the laser ultrasonic technique has the ability to detect the sub-millimeter-scale internal defects in industrial components and engineering structures.

OCIS codes: 140.0140, 160.0160.

Internal defects might cause cracking in power plant components, therefore, harmful internal defects should be detected as early as possible and appropriate treatment should be carried out. Because an ultrasonic wave propagates through opaque materials such as metals very efficiently by means of a simple device, it facilitates the detection of internal defects in opaque materials. Therefore, ultrasonic testing is widely used to inspect whether harmful defects are present and to quantify their size in a wide range of materials, components, and engineering structures. Ultrasonic wave generated by the pulsed laser has received considerable attention since the acoustic pulses have a short pulse duration, typically less than 1.0 μs long, and there is wide application in nondestructive evaluation fields[1,2] and materials characterization[3].

It is expected that the ultrasonic waveforms obtained by laser ultrasonic technique express the conditions of the measured materials more precisely[4], and that this analysis technique has potential for detection of the micrometer scale internal defects. Furthermore, the acoustic waves generated by two laser beams with the same characters have been proved to have the larger amplitude, especially shear wave, which can be applied to the detection of internal defects. The sharp lateral focus of the internal waves, which persists for some depth, suggests that one can use this ideal characteristic to detect internal defects with good spatial resolution. The large shear wave amplitude produced by this method also suggests that defect detection can be carried out by shear to compression mode conversion.

The scattered waveforms produced by the internal defect are dependent on the features of the cylindrical shaped defect. The experimental results of previous literatures[5] have been self-consistent in showing that the waveforms scattered from the internal defect contain an additional component when compared to the incident acoustic pulse. Since the scattered waveform may form the basis of an inside defect sizing and contour technique in metals, it is important that its nature is fully understood. The generation and propagation procession of thermoelastic waves are complex, especially the processes involving the mode conversion phenomena. The finite element method (FEM), adopted in this paper, has many advantages, first of all, it is versatile due to its flexibility in modeling complicated geometry and its availability in obtaining full field numerical solutions. In addition, the method can directly give the enough temporal resolution to resolve the abundant frequency components of the pulse of the scattered bulk wave signals.

The geometry of laser irradiation on a specimen is schematically shown in Fig. 1, the laser beam is assumed to be perpendicular to the surface, where it heats a finite subsurface volume. The spatial mode of the laser beam is assumed to be a Gaussian distribution in the x-direction and a uniform distribution in the z-direction; in addition, the hole on the side wall acts on the internal defect, being assumed to be uniform along the z-direction, so that the three-dimensional Cartesian coordinate system could be reduced to the two dimensions, as shown in Fig. 2.

The incident laser is modeled as a surface heat source, and the equations of motion for the top region are given by

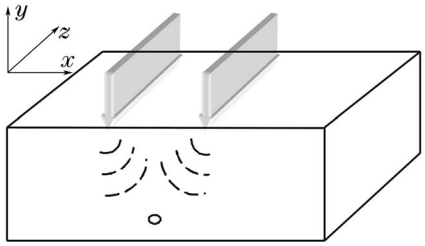

Fig. 1. Schematic diagram of the sample irradiated by two laser beams.

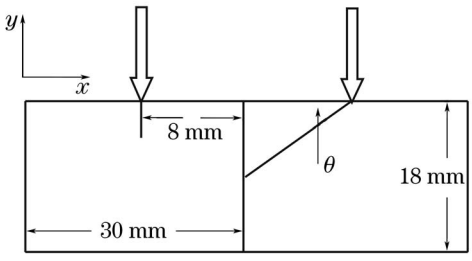

Fig. 2. Cross section of the sample.

$$\rho c_v \frac{\partial T(t,x,y)}{\partial t} - K\left(\frac{\partial^2 T(t,x,y)}{\partial x^2} - \frac{\partial^2 T(t,x,y)}{\partial y^2}\right) = E_0 A(T) h(t) \left[g(x-\bar{x}_1) + g(x-\bar{x}_2)\right], \quad (1)$$

where $T(t,x,y)$ is the temperature field, K is the thermal conductivity, ρ is the mass density, c_v is the specific heat, $A(T)$ is the optical absorptivity of specimen; $g(x-\bar{x}_i)$ and $h(t)$ are the spatial and temporal distribution of the laser pulse, respectively. These two functions can be written as

$$h(t) = \frac{t}{t_0^2} \exp\left(-\frac{t}{t_0}\right), \quad (2)$$

$$g(x-\bar{x}_i) = \exp\left(-\frac{(x-\bar{x}_i)^2}{a_0^2}\right), (i=1,2), \quad (3)$$

where t_0 is the rise time of the laser pulse, a_0 is the half-width of the pulsed laser line source, x_1 and x_2 are the central positions of two laser beams illuminating on the sample.

When the specimen surface is illuminated with a laser pulse with the energy less than the melting threshold of the specimen, a transient displacements field will be excited due to the thermoelastic expansion. In an isotropic body, the displacement satisfies

$$\mu\left(\frac{\partial^2 U_y}{\partial x^2} + \frac{\partial^2 U_y}{\partial y^2}\right) + (\lambda+\mu)\left(\frac{\partial^2 U_y}{\partial x \partial y} + \frac{\partial^2 U_y}{\partial y^2}\right) - \alpha(3\lambda+2\mu)\left(\frac{\partial T}{\partial x} + \frac{\partial T}{\partial y}\right) = \rho \ddot{U}, \quad (4)$$

$$\mu\left(\frac{\partial^2 U_x}{\partial x^2} + \frac{\partial^2 U_x}{\partial y^2}\right) + (\lambda+\mu)\left(\frac{\partial^2 U_x}{\partial x \partial y} + \frac{\partial^2 U_x}{\partial y^2}\right) - \alpha(3\lambda+2\mu)\left(\frac{\partial T}{\partial x} + \frac{\partial T}{\partial y}\right) = \rho \ddot{U}, \quad (5)$$

Where $U(t,x,y)$ is the time-dependent displacements, and the U_x, U_y represent the x- and y-direction displacement, λ, μ are Lamè constants, and α is the thermoelastic expansion coefficient of the isotropic plate material. The free boundary conditions at the two parallel surfaces and the sphere internal surface of the internal defect can be expressed as

$$n \cdot [\sigma - (3\lambda+2\mu)\alpha T(x,y,t) I] = 0, \quad (6)$$

where n is the unit vector normal to the surface, I is the unit tensor and σ is the stress tensor. In addition to the boundary condition, there is also an initial condition

$$U(x,y,t) = \frac{\partial U(x,y,t)}{\partial t} = 0, \qquad t = 0. \quad (7)$$

The thermal expansion is then generated by the imposed temperature field through Eq. (4). The conversion of elastic energy to thermal energy is ignored and the temperature rise is considered to be due to the incident laser only. The calculations are based on the physical properties of an aluminum sample: $\alpha = 2.31 \times 10^{-5}\ \mathrm{K}^{-1}$, $\lambda = 5.81 \times 10^{10}$ Pa; $\mu = 2.61 \times 10^{10}$ Pa; and the temperature dependence parameters such as optical absorptivity, thermal conductive, density and specific heat were given in previous papers[6].

The distortion of the compression arrival peak at 3.14 μs and shear arrival peak at 6.35 μs have been shown in the Fig. 3, which has the pronounced features to help us to understand the influence of the internal defect on the waveform. Figure 4 demonstrates the bulk ultrasonic waveform recorded at the epicenter under the conditions that the internal defect was located in the position of centre axis of the two laser source and the distance between the centres of the sphere-shaped defect to the back surface is kept 6 mm. The location of the defect has been fixed in the finite element model, with the help of the known speeds of compression and shear wave in aluminum, the mode conversion that occurred in the interaction of the bulk ultrasonic wave and the internal defect have been analyzed in this paper.

Measuring the timing of the four more pronounced new features that appear in the Fig. 4 due to the presence of the defect, we can draw a initial conclusion that the first feature occurring at 4.8 μs is the arrival of the compression wave reflected first by the back surface and then by the defect. The second feature occurring at 5.7 μs, labeled dSP, is due to shear to compression mode conversion at the defect, with the scattered compressional wave reaching the transducer before the direct shear wave arrived. Compared with Figs. 4 and 5, we can find that the radii of the internal sphere shaped defects have the obvious influence on the characteristics of the waveform

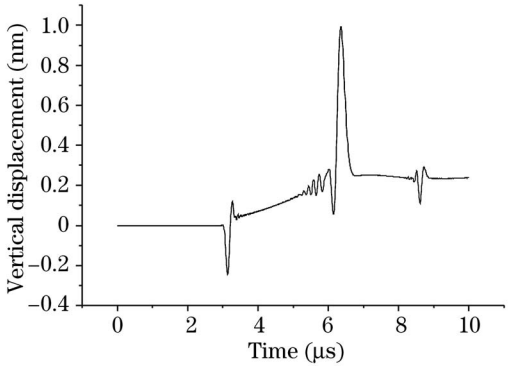

Fig. 3. The bulk wave signal received at the epicenter of the sample without defect.

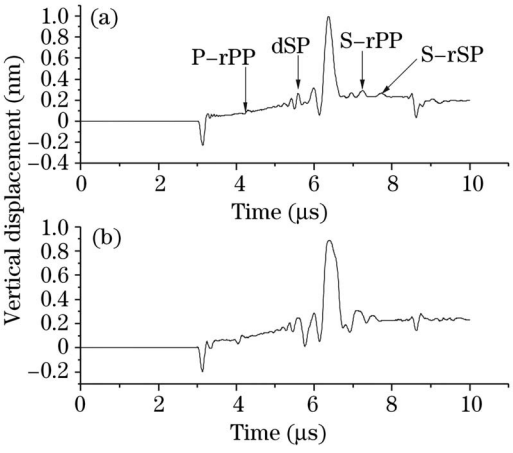

Fig. 4. The bulk wave signal received at the epicenter of the sample with the defect's radii being 0.5 (a) and 1 mm (b) with the center located at y=4 mm.

recorded at the epicenter. So the results suggest that we can further deduce the locations and dimensions of the internal crack using the bulk ultrasonic wave forms generated by two laser beams, which are moving on the top surface of the sample.

Finite element method has provided a viable tool to simulate the complex phenomena of mode conversion occurred in the bulk ultrasonic wave interrogates the internal defect; and the bulk wave generated by the two laser beam has the capacity to identify the internal defect with the sub-millimeter diameter. In addition, in combination with the numerical results of the normalized amplitude of the defect signal on the different defect with varied diameters, the present study can also serve as a basis for the quantitative measurements of inclusions in materials.

X. Ni is the author to whom the correspondence should be addressed, his e-mail address is nxw@mail.njust.edu.cn.

References

1. Q. Shan and R. J. Dewhurst, Appl. Phys. Lett. **62,** 2649 (1993).
2. T. Tanaka and Y. Izawa, Jpn. J. Appl. Phys. **40,** 1477 (2001).
3. B. Q. Xu, Z. H. Shen, X. W. Ni, J. J. Wang, J. F. Guan, and J. Lu, Appl. Phys. Lett. **85,** 2364 (2004).
4. K. Heller, L. J. Jacobs, and J. Qu, NDT&E International **33,** 555 (2000).
5. X. Wang and M. G. Littman, J. Appl. Phys. **80,** 4274 (1996).
6. B. Q. Xu, Z. H. Shen, X. W. Ni, and J. Lu, J. Appl. Phys. **95,** 2116 (2004).